

# A STRUCTURE-FUNCTION SUBSTRATE OF MEMORY FOR SPATIAL CONFIGURATIONS IN MEDIAL AND LATERAL TEMPORAL CORTICES

Shahin Tavakol<sup>1</sup>, Qionglng Li<sup>1</sup>, Jessica Royer<sup>1</sup>, Reinder Vos de Wael<sup>1</sup>, Sara Larivière<sup>1</sup>, Alex Lowe<sup>1</sup>, Casey Paquola<sup>1</sup>, Elizabeth Jefferies<sup>2</sup>, Tom Hartley<sup>2</sup>, Andrea Bernasconi<sup>1</sup>, Neda Bernasconi<sup>1</sup>, Jonathan Smallwood<sup>2</sup>, Veronique Bohbot<sup>3</sup>, Lorenzo Caciagli<sup>4\*</sup>, Boris Bernhardt<sup>1\*</sup>

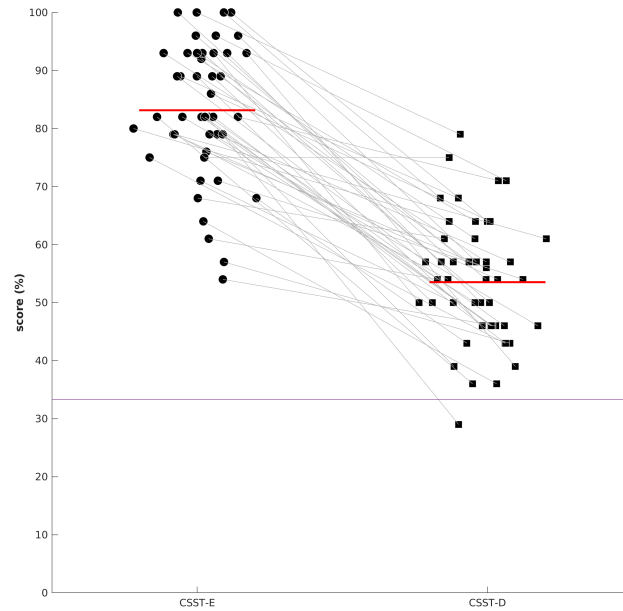
- 1) *McConnell Brain Imaging Centre, Montreal Neurological Institute and Hospital, McGill University, Montreal, Quebec, Canada*
- 2) *University of York, York, UK*
- 3) *Douglas Mental Health University Institute, McGill University, Montreal, Quebec, Canada*
- 4) *Department of Bioengineering, University of Pennsylvania, Philadelphia, USA*

## SUPPLEMENTARY METHODS

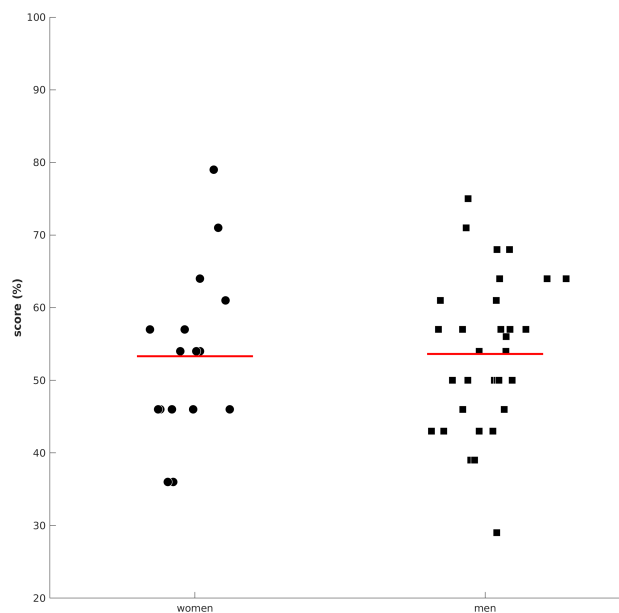
### *Structural MRI processing*

*Hippocampal subfield surface mapping.* We harnessed a validated approach for the segmentation of hippocampal subfields, generation of surfaces running through the core of each subfield, and surface-based “unfolding” of hippocampal features (Caldairou, et al., 2016; Bernhardt, et al., 2016; Vos de Wael, et al., 2018). In brief, each participant’s native-space T1w image underwent automated correction for intensity non-uniformity, intensity standardization, and linear registration to the MNI152 template. Images were subsequently processed using a multi-template surface-patch algorithm (Caldairou, et al., 2016), which automatically segments the left and right hippocampal formation into subiculum, CA1-3, and CA4-DG. An open-access database of manual subfield segmentations and corresponding high resolution 3T MRI data (Kulaga-Yoskovitz, et al., 2015) was used for algorithm training. A Hamilton-Jacobi approach (Kim, et al., 2014) generated a medial surface sheet representation running along the central path of each subfield and surfaces were parameterized using a spherical harmonics framework with a point distribution model (Styner, et al., 2006). For each subfield surface vertex, we then calculated columnar volume as a marker of local grey matter (Kim, et al., 2014). During data analysis, vertex-wise projections of hippocampal columnar volume underwent surface-wide smoothing (FWHM=10) using SurfStat for Matlab (MathWorks, R2019b).

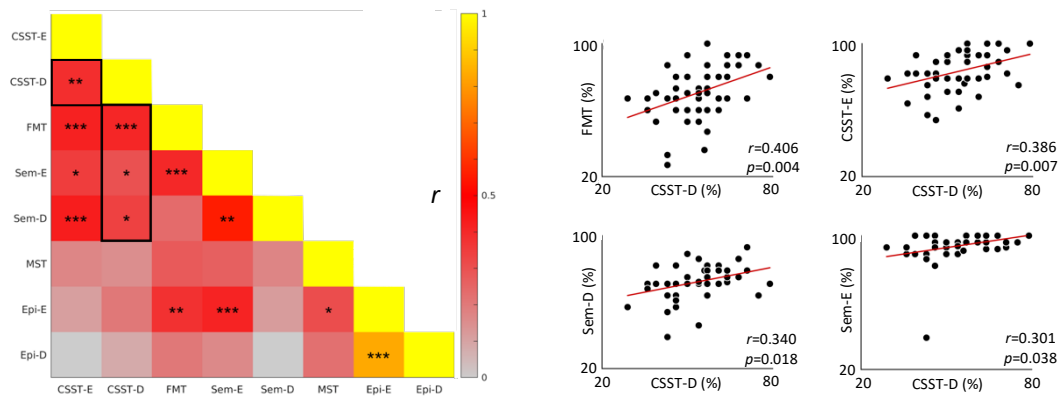
## SUPPLEMENTARY FIGURES



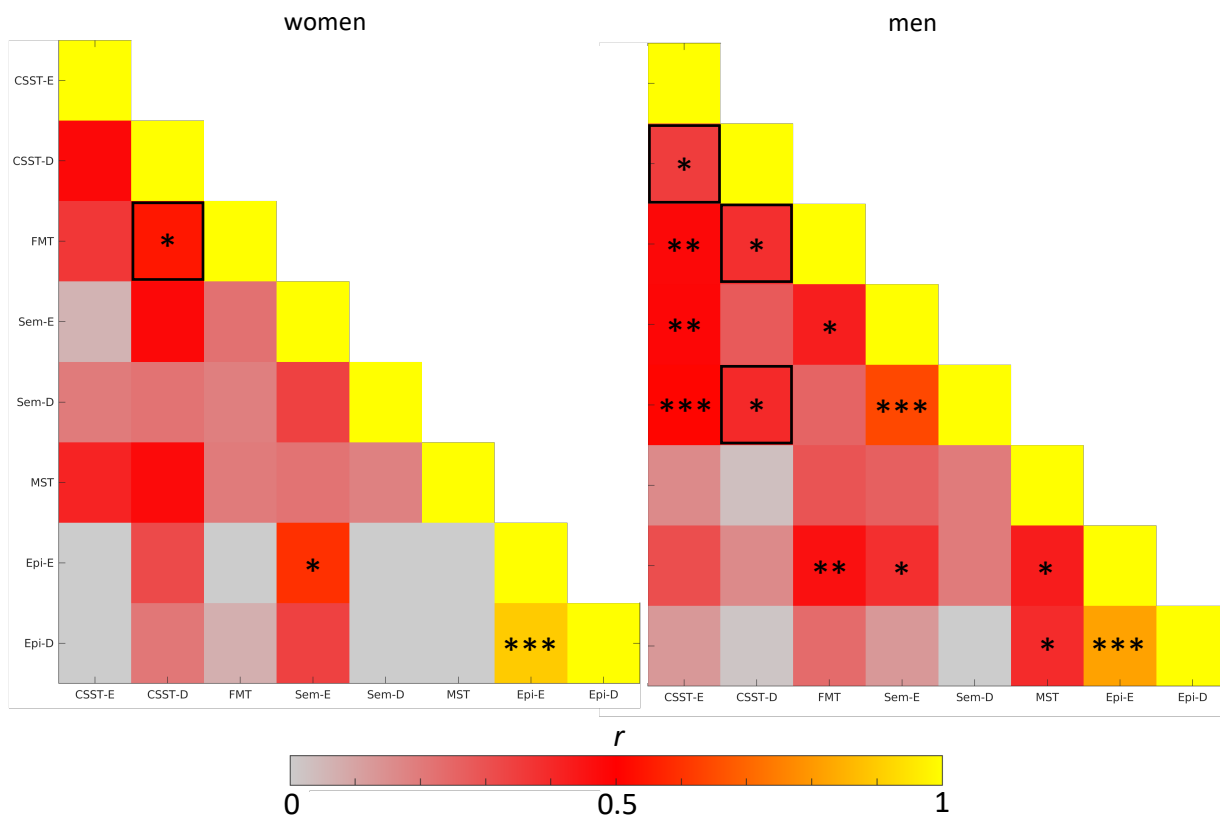
**Supplemental Figure 1** | Participants scored significantly higher on the CSST-E ( $83.1 \pm 11.3\%$ ) compared to the CSST-D ( $53.5 \pm 10.7$ ) as evidenced by a two-tailed paired student t-test ( $t=16.8$ ,  $p<0.001$ ). Red horizontal lines show distribution means. Chance level performance is depicted as a horizontal line (33.33%). Participants scored significantly higher than chance level on each condition (CSST-E:  $t=30.4$ ,  $p<0.001$ ; CSST-D:  $t=13.1$ ,  $p<0.001$ ).



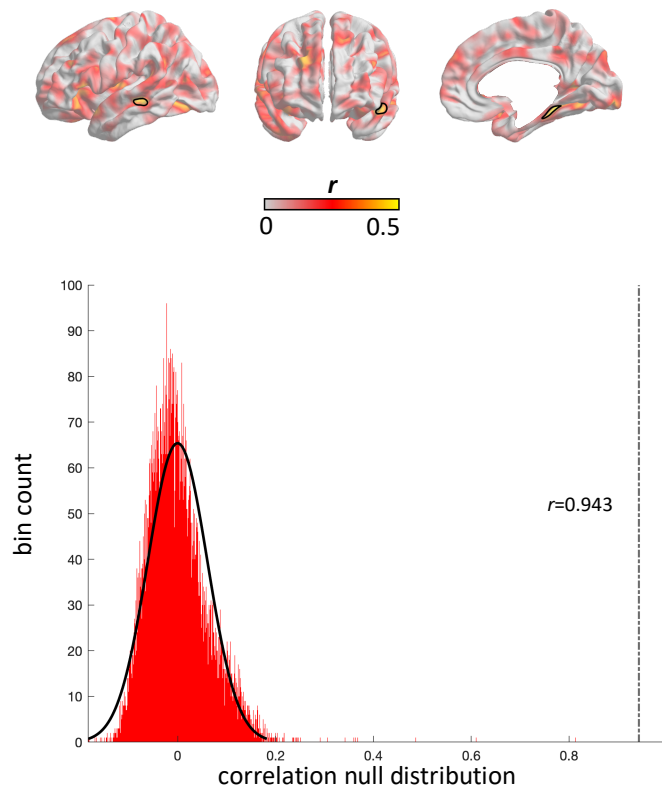
**Supplemental Figure 2** | In order to assess whether variability in the results is driven by middle-aged participants, we assessed whether individuals above 35 years of age performed similarly to younger adults. No age-related differences were observed in either sex group (older women:  $54.5 \pm 14.4\%$ , young women:  $52.9 \pm 11.3\%$ ,  $t=0.227$ ,  $p=0.823$ ; older men:  $50.4 \pm 7.5\%$ , young men:  $54.5 \pm 11.0\%$ ,  $t=0.918$ ,  $p=0.366$ ). Thus, we combined data across age strata in each group and compared scores. We observed no sex differences in CSST-D performance (women:  $53.3 \pm 11.7\%$ ; men:  $53.6 \pm 10.4\%$ ;  $t=0.094$ ,  $p=0.925$ ).



**Supplemental Figure 3** | *left*: correlation matrix of performance across all tasks, including easy conditions. Outlined area shows tasks with which CSST-D shows significant associations ( $*p<0.05$ ;  $**p<0.01$ ;  $***p<0.005$ ). *right*: scatter plot of most significant associations with other tasks (FMT: Four Mountains Task; CSST-D/E: Conformational Shift Spatial Task-Difficult/Easy; Sem-D/E: Semantic Task-Difficult/Easy; Epi-D/E: Episodic Difficult/Easy; MST: Mnemonic Similarity/Discrimination Task)

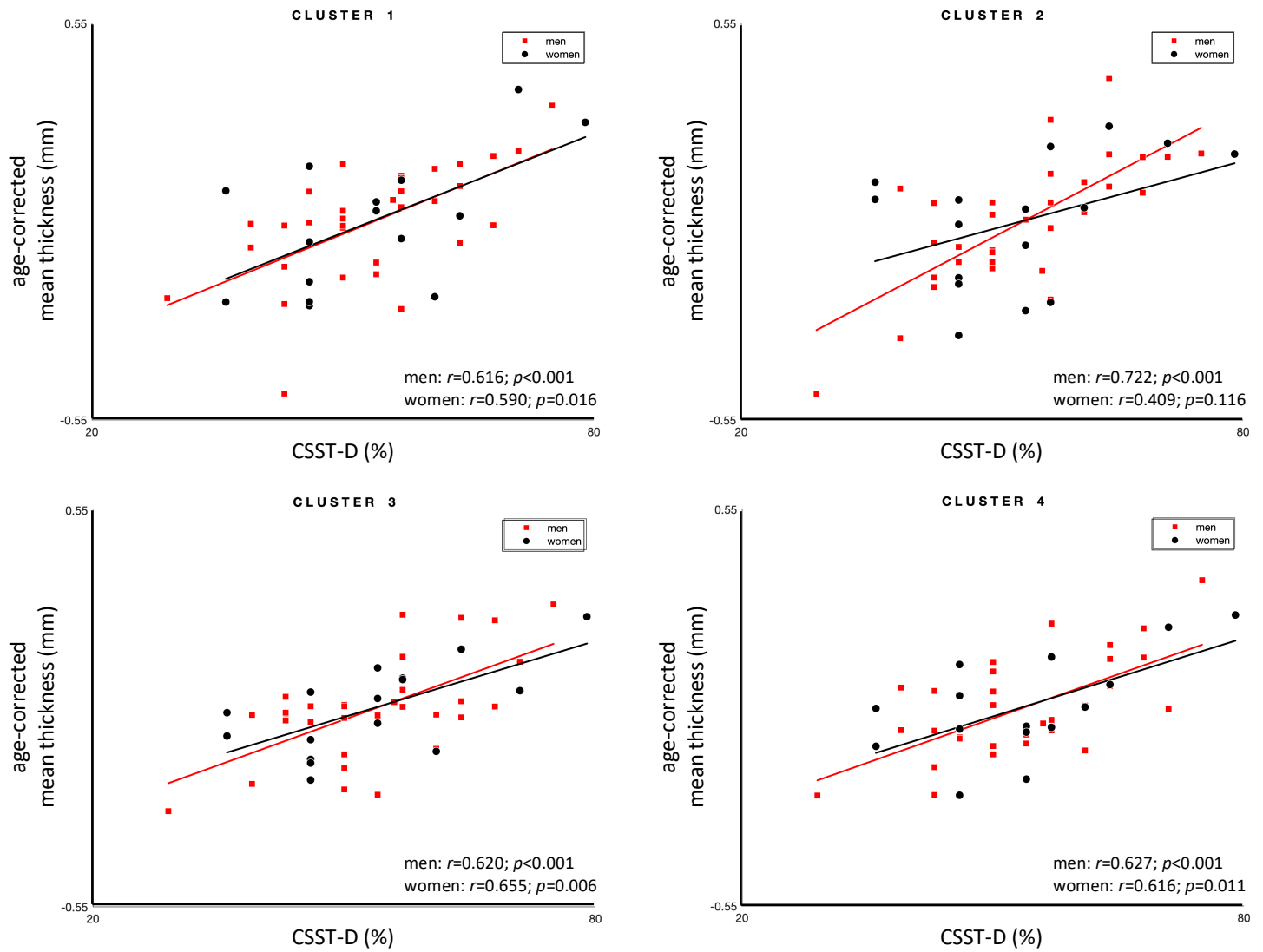


**Supplemental Figure 4** | Correlation matrix of performance across all tasks for women and men. Outlined areas show tasks with which CSST-D shows significant associations ( $*p<0.05$ ;  $**p<0.01$ ;  $***p<0.005$ ). (FMT: Four Mountains Task; CSST-D/E: Conformational Shift Spatial Task-Difficult/Easy; Sem-D/E: Semantic Task-Difficult/Easy; Epi-D/E: Episodic Difficult/Easy; MST: Mnemonic Similarity/Discrimination Task)

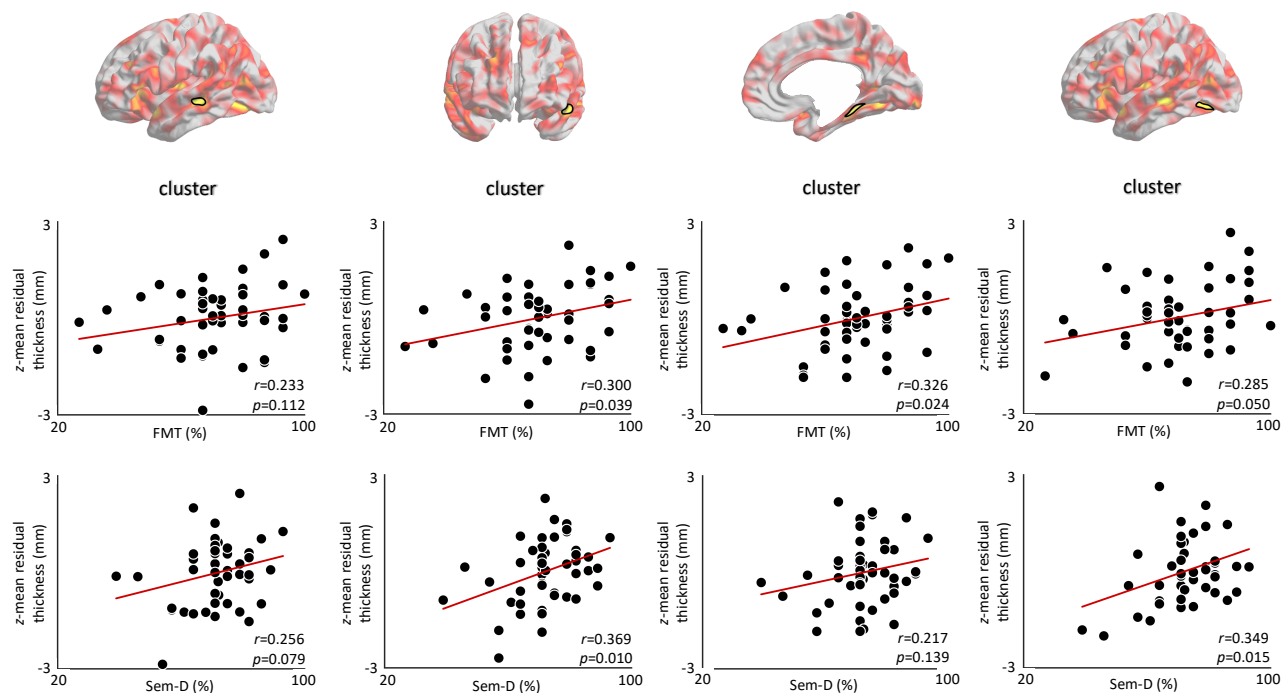


**Supplemental Figure 5 | top panel:** Product-moment correlation coefficients of CSST-D performance on cortical thickness after regressing out age and sex for right-handed participants ( $n=44$ ). Highlighted clusters denote regions of significant association after multiple comparisons correction ( $p_{FWE}<0.05$ ). **bottom panel:** a non-parametric null distribution was generated by correlating the *CSST-D x cortical thickness* statistical  $t$  map with 10,000 permuted  $t$  maps of *right-handed only CSST-D x cortical thickness*. Actual correlation between original maps is shown by the dashdotted line ( $r=0.943$ , non-parametric  $p<0.001$ ).

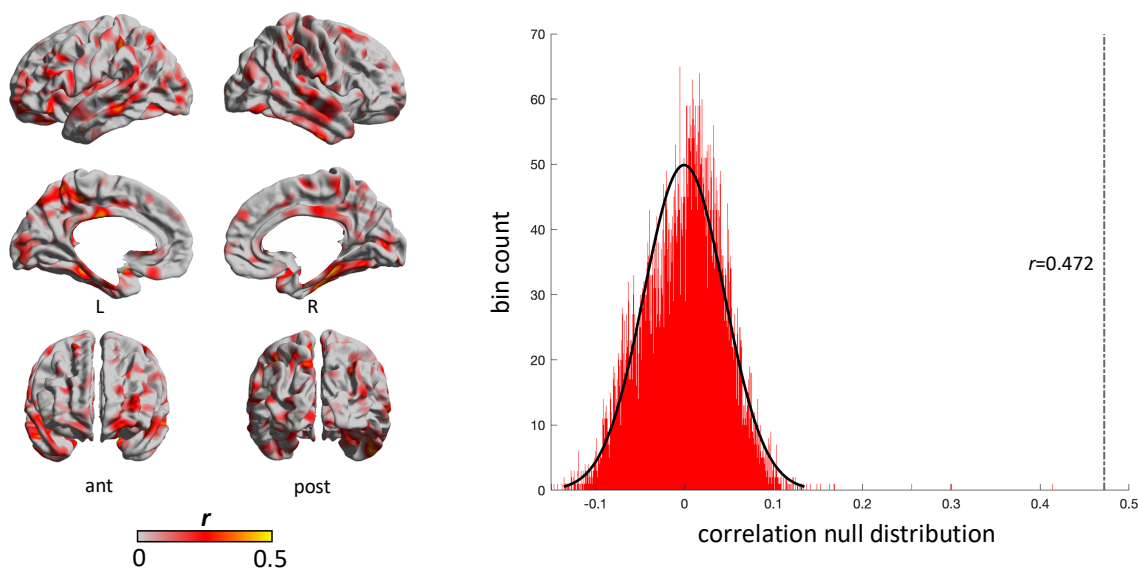




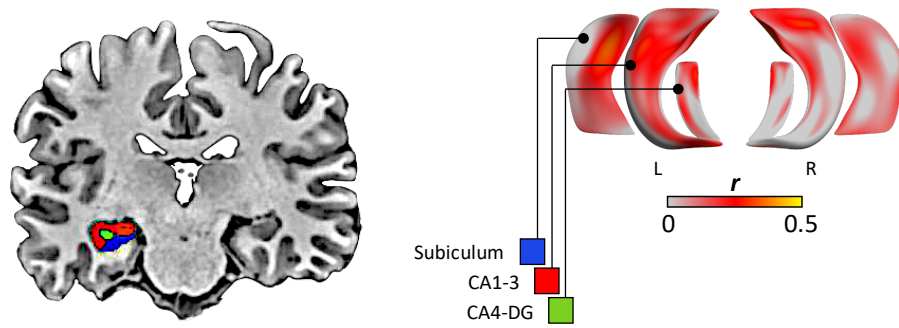
**Supplemental Figure 6** | Controlling for age, we observed moderate-to-high associations between average cortical thickness and CSST-D scores for all clusters in men and women.



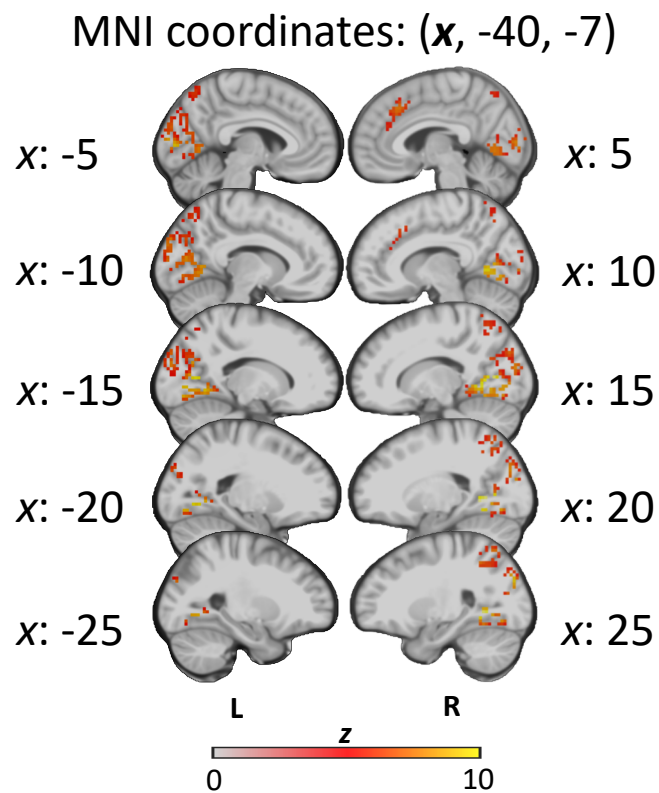
**Supplemental Figure 7** | Cluster-wise associations between cortical thickness and scores for FMT (top row scatterplots) and Sem-D (bottom row scatterplots). Correlation coefficients ranged between  $r=0.233$ - $0.326$  for FMT (mean effect of 0.353), and between  $r=0.217$ - $0.369$  for Sem-D (mean effect of 0.373).



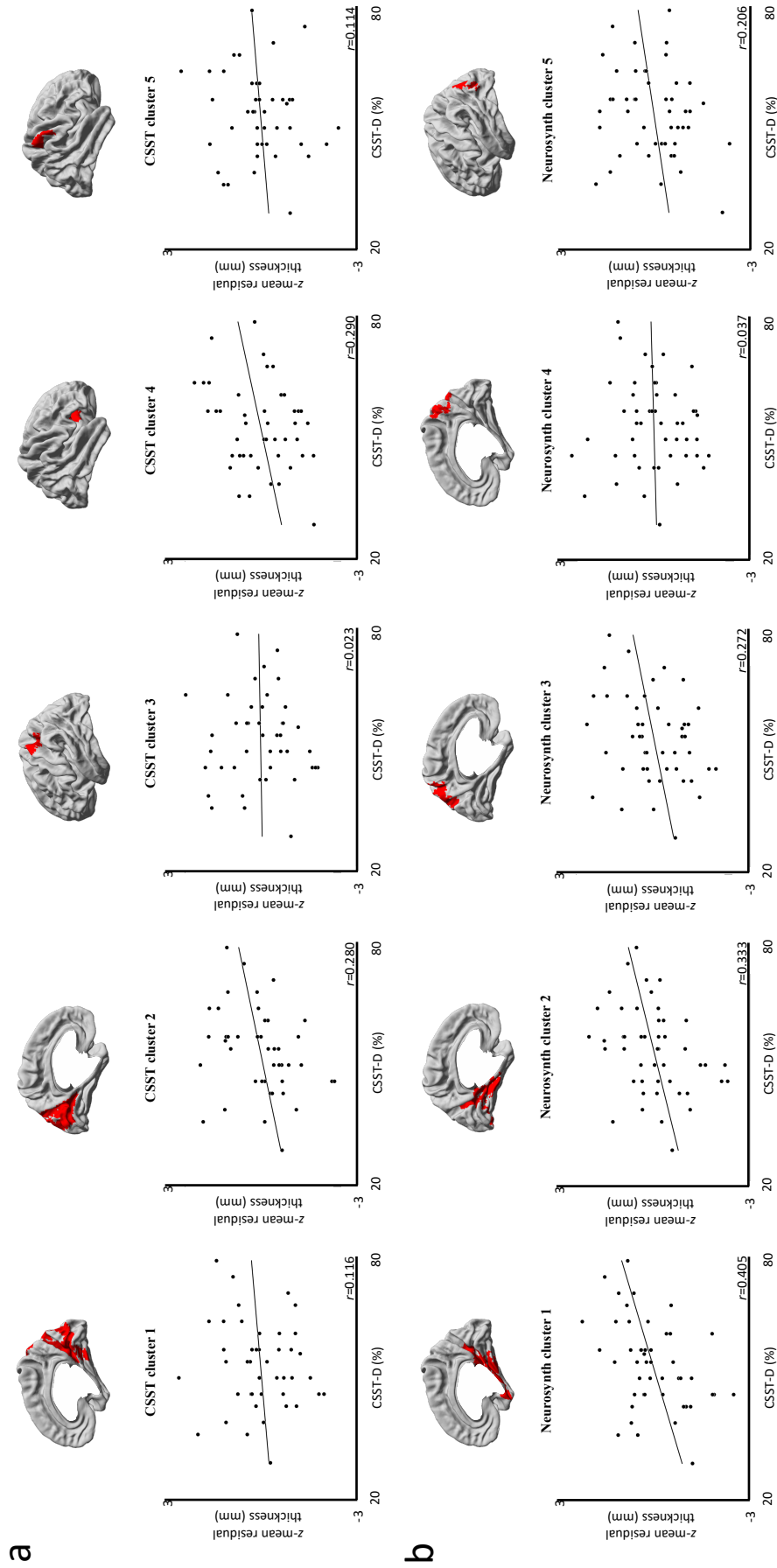
**Supplemental Figure 8** | **left panel:** Product-moment correlation coefficients of FMT performance on cortical thickness after regressing out age and sex. **right panel:** a non-parametric null distribution was generated by correlating the *CSST-D*  $\times$  cortical thickness statistical  $t$  map with 10,000 permuted  $t$  maps of *FMT*  $\times$  cortical thickness. Actual correlation between original maps is shown by the dashdotted line ( $r=0.472$ , non-parametric  $p<0.001$ ).



**Supplemental Figure 9** | **left panel:** coronal section of the brain showing the hippocampal subfields. **right panel:** uncorrected associations between CSST-D score and columnar volume shown on hippocampal subfield surfaces after regressing out age and sex.



**Supplemental Figure 10** | Group-level volumetric activation map for the contrast between retrieval and encoding.



**Supplemental Figure 11 | Associations between cortical thickness and CSST-D performance for functionally-defined clusters after controlling for age and sex. a** Top 5 largest clusters for group level ( $n=44$ ) CSST activation for *retrieval-vs.-encoding* weighted contrast ( $r=0.023-0.290$ ). **b** Top 5 largest clusters for Neurosynth-derived coactivations for the term “navigation” ( $r=0.037-0.405$ ).

FMT	0.406			
Sem-D	0.340	0.237		
MST	0.150	0.278	0.172	
Epi-D	0.083	0.206	-0.058	0.224
	CSST-D	FMT	Sem-D	MST

**Supplemental Table 1** | Product-moment correlation coefficients of task performance scores (see **Figure 1b**)

	successful	unsuccessful
CSST-E	23 ± 3 (15-28)	5 ± 3 (0-13)
CSST-D	15 ± 3 (8-22)	13 ± 3 (6-20)
Total	38 ± 5 (28-50)	18 ± 5 (6-28)

**Supplemental Table 2** | Number of successful and unsuccessful trials in the each condition of the CSST reported as the mean ± SD (range) .

MNI x,y,z {mm}	peak T	peak p(unc)	peak p(FWE-corr)
18 -64 5	14.87	<0.001	<0.001
21 -58 -1	14.52	<0.001	<0.001
12 -58 2	11.74	<0.001	<0.001
-15 -67 8	11.24	<0.001	<0.001
-18 -76 -4	11.16	<0.001	<0.001
-21 -64 -4	10.7	<0.001	<0.001
33 23 2	9.68	<0.001	<0.001
39 20 -13	7.13	<0.001	0.001
-39 -22 59	9.54	<0.001	<0.001
-39 -37 41	7.99	<0.001	<0.001
-33 -16 65	7.97	<0.001	<0.001
36 -49 50	9.17	<0.001	<0.001
27 -52 47	9.01	<0.001	<0.001
24 -67 59	8.2	<0.001	<0.001
6 26 41	8.46	<0.001	<0.001
6 38 23	6.37	<0.001	0.008
45 -28 47	8.19	<0.001	<0.001
42 -37 47	7.91	<0.001	<0.001
51 -19 44	7.19	<0.001	0.001
45 32 23	8.05	<0.001	<0.001
-9 -70 53	7.14	<0.001	0.001
-12 -76 47	6.52	<0.001	0.005

**Supplemental Table 3** | Group-level volumetric statistics for contrast between retrieval and encoding across pooled CSST-E and CSST-D trials.